

# Robust Traffic Control Using a First Order Macroscopic Traffic Flow Model

Hao Liu<sup>a</sup>, Christian Claudel<sup>a</sup>, and Randy Machemehl<sup>a</sup>

<sup>a</sup>Department of Civil, Architectural and Environmental Engineering, University of Texas Austin, USA

**Abstract**—Traffic control is at the core of research in transportation engineering because it is one of the best practices for reducing traffic congestion. It has been shown in recent years that the traffic control problem involving Lighthill-Whitham-Richards (LWR) model can be formulated as a Linear Programming (LP) problem given that the corresponding initial conditions and the model parameters in the fundamental diagram are fixed. However, the initial conditions can be uncertain when studying actual control problems. This paper presents a stochastic programming formulation of the boundary control problem involving chance constraints, to capture the uncertainty in the initial conditions. Different objective functions are explored using this framework, and case studies for both a single highway link and a small network are conducted. In addition, the optimal results are validated with Monte Carlo simulation.

**Index Terms**—Traffic control, linear programming, stochastic programming, chance constraints, optimal control

## I. INTRODUCTION

**T**RAFFIC congestion is a global issue which is expected to become worse in the next decades as cities and populations continue to grow. As the number of vehicles increases, both people and the environment are severely affected in terms of congestion and pollution, which translates into a waste of time and money. Therefore, reducing traffic congestion is a critical issue to our human society. There are a number of ways in which congestion could be reduced, such as increasing the road capacity and decreasing user demand. However, these methods are expensive or sometimes impractical.

The traffic flow is usually modeled by deterministic Partial Differential Equations (PDEs) [1], [2], [3], [4]. In addition, there has been much attention paid to stochastic modeling of traffic flow. A common way to construct a stochastic traffic flow model is adding ‘noise’ into a selected deterministic model. The stochastic models are advantageous for both traffic state estimation [5], [6], [7] and traffic control [8]. However, these methods only considered freeway segments shorter than 2 km. In order to overcome this drawback, a general approach [9], [10] to estimate traffic state without the need for the calibration of fundamental diagram parameters was proposed. More recently, [11] pointed out the inconsistency between mean dynamics of the stochastic model and the original dynamics, and a general stochastic model considering the random state dependent headways was developed to address

this issue.

Some promising techniques used to mitigate traffic congestion, such as traffic congestion forecasting and traffic flow control, are based on PDE-based flow models. The Kalman Filter [12] and Autoregressive Integrated Moving Average model [13] are the most frequently used methods for congestion forecasting in the past decade and other alternatives, such as vehicle-to-vehicle communication, machine learning [14], [15], [16], [17] have been developed in recent years. Besides these traffic congestion forecasting techniques, numerous traffic control methodologies [18], [19], [20] have been developed in the past decades. For example, ramp metering, which regulates the flow of traffic, is a widespread traffic control method. ALINER [21], which employs the linear state feedback, is one of the control algorithms used for ramp metering, and it has been used around the world. An asymmetric cell transmission model (ACTM) was proposed in [22] as a ramp metering control method; this model yields a global optimal solution to a nonlinear problem by solving a linear program under certain conditions. PDEs can also be used as flow models, for example in the references [23], [24], [25], [26], in which PDE models are discretized into ODEs to use methods [27] to find the optimal solution. A new control method in [20] does not require any discretization or approximation of the model. This method shows that the traffic control problem can be posed as a Linear Programming (LP) problem under the triangular fundamental diagram for the traffic flow modeled by the Lighthill-Whitham-Richards (LWR) PDE. This framework significantly reduces computational complexity over standard traffic control computational methods.

In the control algorithm developed in [20], the initial conditions and the parameters of the fundamental diagram are known and fixed. In reality, there are no reliable strategies to capture the precise densities on a highway link, and the measurement of the traffic density depends on indirect measurements of other variables such as speed and flow [28]. Both deterministic approaches [4], [29] and stochastic approaches [30], [31] have been proposed to make the density estimation more dependable. Also, the parameters in the fundamental diagram can be affected by factors such as drive behavior, weather condition, and are stochastic in nature. Numerous studies have investigated the stochastic nature of freeway capacity [32], [33], [34]. Unexpected consequences may be caused by the neglect of the uncertainty associated with each of these quantities. For example, if the critical density used in the control method is larger than its real value while the free flow speed and jam density

are accurate, the capacity of the highway link, which is the product of free flow speed and critical density, would be overestimated. Through the control method from [20], the optimal outflows of the highway link for the objective function of maximizing total outflow are equal to the given capacity. With the given capacity being larger than its real value, some vehicles could not get through the link and would cause congestion if this control method was used without considering uncertainty. Thus, robust control which considers the uncertainty associated with each of these quantities is necessary for the traffic control problem. In [35], a framework which only assumes bounds on the uncontrolled components of the initial and boundary conditions was developed to perform the robust traffic control. But the optimal solution from this method is too conservative. To overcome this drawback, in this paper, we propose a new robust traffic control framework through a stochastic program with chance constraints rather than a linear program with bounds constraints.

The objective of this paper is to study the effect of uncertainties in initial densities on the traffic control. The main contributions of this paper are: 1. We propose a stochastic program with chance constraints to consider the uncertainty in the initial conditions. In the stochastic program formulation, some relaxations are made in order to convert these chance constraints into deterministic form. The proposed model could be extended to be applicable to networked systems of first order hyperbolic PDEs involving a convex flux function with more effort; 2. The effectiveness of the proposed model are demonstrated through case studies for both a single highway link and a network; 3. The results from Monte Carlo simulation are compared to the relaxation solutions, and they agree with each other well.

The rest of this paper is organized as follows. Section 2 reviews the framework of the LP formulation for the traffic control problem. Section 3 presents the stochastic optimization model, which takes into consideration the uncertainty of the initial densities, and a case study for a single highway link. Section 4 proposes the model and executes a case study for a highway network. In section 5, Monte Carlo simulation results were compared to the model proposed in Section 3. Section 6 summarizes the work and potential future work.

## II. LP MODEL DEFINITION

This section covers an LP framework, proposed in [20], [35], for the traffic control problem since the model proposed later is built on this model. The organization of this section is as follows: part A introduces the traffic flow model; by using Lax-Hopf formula, part B shows the Moskowitz solutions, derived in [36], [37], associated with each value condition; such solutions have to satisfy the compatibility condition to ensure that the true solutions equal the true value conditions at corresponding points, part C presents the mathematical form of this compatibility condition. For details regarding the derivation and proof, we refer readers to references [20], [38], [39].

### A. Traffic Flow Models

Lighthill-Whitham-Richards (LWR) PDE model [1], [2] is one of the most commonly used models to depict the evolution of traffic flow,

$$\frac{\partial \rho(t, x)}{\partial t} + \frac{\partial \psi(\rho(t, x))}{\partial x} = 0 \quad (1)$$

where  $\rho(t, x)$  is the density of the point  $x$  away from a reference point at time  $t$ ,  $\psi$  is the concave Hamiltonian, which is used to denote the experimental relationship between flow and density. For simplicity, a triangular fundamental diagram is used to present the relationship between flow and density,

$$\psi(\rho) = \begin{cases} v_f \rho & \rho \in [0, \rho_c] \\ w(\rho - \rho_m) & \rho \in [\rho_c, \rho_m] \end{cases} \quad (2)$$

where  $v_f$  is the free flow speed,  $w$  is the congestion speed,  $\rho_c$  is the critical density where the flow is maximum,  $\rho_m$  is the jam density, where the flow is zero due to the total congestion. Those parameters are dependent and the relationship between them can be expressed as,

$$\rho_c = \frac{-w\rho_m}{v_f - w} \quad (3)$$

Alternatively, the traffic flow can be modeled by a scalar function  $M(t, x)$ , known as the Moskowitz function [40], which represents the index of the vehicle at  $(t, x)$ . The relationship between the Moskowitz function and density and flow can be expressed as,

$$\rho(t, x) = -\frac{\partial M}{\partial x}, \quad q(t, x) = \frac{\partial M}{\partial t} \quad (4)$$

Therefore, another traffic flow model, Hamilton-Jacobi (H-J) PDE, can be obtained from the integration of the LWR PDE model (1) in space,

$$\frac{\partial M(t, x)}{\partial t} - \psi\left(-\frac{\partial M(t, x)}{\partial x}\right) = 0 \quad (5)$$

For the purposes of this work, the spatial domain  $[\xi, \chi]$ , where  $\xi$  is the upstream boundary and  $\chi$  is the downstream boundary, were divided evenly into  $k_{max}$  segments; the time domain  $[0, t_{max}]$ , where  $t_{max}$  is the simulation time, were divided evenly into  $n_{max}$  segments. Also, we defined  $K = \{1, \dots, k_{max}\}$  and  $N = \{1, \dots, n_{max}\}$ . The piecewise affine initial condition  $M_k(t, x)$ , upstream boundary condition  $\gamma_n(t, x)$ , and downstream boundary condition  $\beta_n(t, x)$  in terms of the Moskowitz function are defined as follows,

$$M_k(t, x) = \begin{cases} -\sum_{i=1}^{k-1} \rho(i)X \\ -\rho(k)(x - (k-1)X), & \text{if } t = 0 \\ +\infty, & \text{and } x \in [(k-1)X, kX] \\ & \text{otherwise} \end{cases} \quad (6)$$

$$\gamma_n(t, x) = \begin{cases} \sum_{i=1}^{n-1} q_{in}(i)T \\ +q_{in}(n)(t - (n-1)T), & \text{if } x = \xi \\ +\infty, & \text{and } t \in [(n-1)T, nT] \\ & \text{otherwise} \end{cases} \quad (7)$$

$$\beta_n(t, x) = \begin{cases} \sum_{i=1}^{n-1} q_{out}(i)T \\ + q_{out}(n)(t - (n-1)T) \\ - \sum_{k=1}^{k_{max}} \rho(k)X, & \text{if } x = \chi \\ & \text{and } t \in [(n-1)T, nT] \\ +\infty, & \text{otherwise} \end{cases} \quad (8)$$

where  $X$  and  $T$  are the length for the spatial segment and time segment, respectively,  $\rho(i)$  is the initial density for the  $i$ th spatial segment,  $q_{in}(i)$  and  $q_{out}(i)$  are the inflow and outflow, respectively, for the  $i$ th time segment at boundaries. In these conditions, we chose the appropriate initial and boundary segment length and assumed the initial density and boundary flow conditions in the corresponding segments are constants. To ensure that the time steps and space steps of the problem are consistent with the characteristic velocities of traffic (on the order of  $v_f$ ), we choose the segment length and time step  $T$  such as  $|v_f T / X| < 1$ . Note that this condition is similar to the classical Courant-Friedrichs-Lewy (CFL) condition used for solving discretized PDEs using some first order numerical schemes, though our numerical scheme is unconditionally stable (and exact) and larger time steps are allowable.

### B. Moskowitz Solutions

The Barron-Jensen/Frankowska (B-J/F) solution [41], [42] was incorporated in to solve the H-J equation. The B-J/F solutions are fully characterized by the Lax-Hopf formula.

**Definition 1 (Value Condition):** A value condition  $c(\cdot, \cdot)$  is a lower semicontinuous function defined on a subset of  $[0, t_{max}] \times [\xi, \chi]$ .

In the following, all of the initial conditions and boundary conditions are regarded as value conditions.

**Proposition 1 (Lax-Hopf Formula):** Let  $\psi(\cdot)$  be a concave and continuous Hamiltonian, and let  $c(\cdot, \cdot)$  be a value condition. The B-J/F solution  $M_c(\cdot, \cdot)$  to (5) associated with  $c(\cdot, \cdot)$  is defined [43], [44], [45] by

$$M_c(t, x) = \inf_{(u, T) \in (\varphi^*) \times R_+} (c(t - T, x + Tu) + T\varphi^*(u)) \quad (9)$$

where  $\varphi^*(\cdot)$  is the Legendre-Fenchel transform of an upper semicontinuous Hamiltonian  $\psi(\cdot)$ , which is given by,

$$\varphi^*(u) := \sup_{p \in \text{Dom}(\psi)} [p \cdot u + \psi(p)] \quad (10)$$

Until now, the explicit Moskowitz solution from the defined value conditions (6)-(8) using Lax-Hopf formula (9) can be expressed as (11)-(13) shown in the next page. For readers

interested in the derivation, see [36], [37].

$$M_{M_k}(t, x) = \begin{cases} +\infty, & \text{if } x \leq (k-1)X + tw \\ & \text{or } x \geq kX + v_f t \end{cases} \quad (11a)$$

$$- \sum_{i=1}^{k-1} \rho(i)X + \rho(k)(tv_f + (k-1)X - x), \quad \text{if } x \geq (k-1)X + v_f t \quad (11b)$$

$$- \sum_{i=1}^{k-1} \rho(i)X + \rho_c(tv_f + (k-1)X - x), \quad \text{and } x \leq kX + v_f t \quad (11c)$$

$$- \sum_{i=1}^{k-1} \rho(i)X + \rho(k)(tw + (k-1)X - x), \quad \text{and } x \geq (k-1)X + tw \quad (11d)$$

$$- \rho_m tw, \quad \text{and } \rho(k) \geq \rho_c \quad (11e)$$

$$- \sum_{i=1}^k \rho(i)X + \rho_c(tw + kX - x), \quad \text{and } x \leq kX + tv_f$$

$$+ \rho_c(tw + kX - x), \quad \text{and } x \geq kX + tw$$

$$- \rho_m tw, \quad \text{and } \rho(k) \geq \rho_c$$

$$M_{\gamma_n}(t, x) = \begin{cases} +\infty, & \text{if } t \leq (n-1)T + \frac{x - \xi}{v_f} \end{cases} \quad (12a)$$

$$\sum_{i=1}^{n-1} q_{in}(i)T + q_{in}(n)(t - \frac{x - \xi}{v_f} - (n-1)T), \quad \text{if } t \geq (n-1)T + \frac{x - \xi}{v_f} \quad (12b)$$

$$t - \frac{x - \xi}{v_f} - (n-1)T, \quad \text{and } t \leq nT + \frac{x - \xi}{v_f}$$

$$\sum_{i=1}^n q_{in}(i)T + \rho_c v_f (t - \frac{x - \xi}{v_f} - nT), \quad \text{otherwise} \quad (12c)$$

$$M_{\beta_n}(t, x) = \begin{cases} +\infty, & \text{if } t \leq (n-1)T + \frac{x - \chi}{w} \end{cases} \quad (13a)$$

$$- \sum_{k=1}^{k_{max}} \rho(k)X + \sum_{i=1}^{n-1} q_{out}(i)T + q_{out}(n)(t - \frac{x - \chi}{w} - (n-1)T) - \rho_m(x - \chi), \quad \text{if } t \geq (n-1)T + \frac{x - \chi}{w} \quad (13b)$$

$$- \sum_{k=1}^{k_{max}} \rho(k)X + \sum_{i=1}^n q_{out}(i)T + \rho_c v_f (t - nT - \frac{x - \chi}{w}), \quad \text{and } t \leq nT + \frac{x - \chi}{w}$$

$$- \sum_{k=1}^{k_{max}} \rho(k)X + \rho_c v_f (t - nT - \frac{x - \chi}{w}), \quad \text{otherwise} \quad (13c)$$

### C. Linear Constraints

The Moskowitz solutions (11)- (13) show that each value condition generates one solution at a certain point in the domain of value conditions, these solutions have to satisfy the compatibility condition to ensure that the true solution is equal to the true value condition (make the solution compatible with the value condition). This part shows that the compatibility condition can be characterized by a set of

linear constraints.

The Lax-Hopf formula (9) leads to the inf-morphism property [43].

*Proposition 2 (Inf-morphism Property):* Let the value condition  $c(\cdot, \cdot)$  be minimum of a finite number of lower semicontinuous functions:

$$\forall(t, x) \in [0, t_{max}] \times [\xi, \chi], \quad c(t, x) := \min_{j \in J} c_j(t, x) \quad (14)$$

The corresponding solution  $M_c(\cdot, \cdot)$  can be decomposed [43], [44] as

$$\forall(t, x) \in [0, t_{max}] \times [\xi, \chi], \quad M_c(t, x) := \min_{j \in J} M_{c_j}(t, x) \quad (15)$$

Based on the *Inf-morphism* property, the Moskowitz solutions (11)-(13) have to satisfy the compatibility conditions [36].

*Proposition 3 (Compatibility Conditions):* Use the value condition  $c(t, x)$  and the corresponding solution in *Proposition 2*. The equality  $\forall(t, x) \in \text{Dom}(c), M_c(t, x) = c(t, x)$  is valid if and only if the inequalities below are satisfied,

$$M_{c_j}(t, x) \geq c_i(t, x), \quad \forall(t, x) \in \text{Dom}(c_i), \forall(i, j) \in J^2 \quad (16)$$

These constraints are linear in terms of initial and boundary conditions and can be expanded as [20], [38], [39],

$$\begin{cases} M_{M_k}(0, x_p) \geq M_p(0, x_p) & \forall(k, p) \in K^2 \\ M_{M_k}(pT, \chi) \geq \beta_p(pT, \chi) & \forall k \in K, \quad \forall p \in N \\ M_{M_k}(\frac{\chi - x_k}{v_f}, \chi) \geq \beta_p(\frac{\chi - x_k}{v_f}, \chi) & \forall k \in K, \quad \forall p \in N \\ \text{s.t. } \frac{\chi - x_k}{v_f} \in [(p-1)T, pT] \\ M_{M_k}(pT, \xi) \geq \gamma_p(pT, \xi) & \forall k \in K, \quad \forall p \in N \\ M_{M_k}(\frac{\xi - x_{k-1}}{w}, \xi) \geq \gamma_p(\frac{\xi - x_{k-1}}{w}, \xi) & \forall k \in K, \quad \forall p \in N \\ \text{s.t. } \frac{\xi - x_{k-1}}{w} \in [(p-1)T, pT] \end{cases} \quad (17)$$

$$\begin{cases} M_{\gamma_n}(pT, \xi) \geq \gamma_p(pT, \xi) & \forall(n, p) \in N^2 \\ M_{\gamma_n}(pT, \chi) \geq \beta_p(pT, \chi) & \forall(n, p) \in N^2 \\ M_{\gamma_n}(nT + \frac{\chi - \xi}{v_f}, \chi) \geq \beta_p(nT + \frac{\chi - \xi}{v_f}, \chi) & \forall(n, p) \in N^2 \\ \text{s.t. } nT + \frac{\chi - \xi}{v_f} \in [(p-1)T, pT] \end{cases} \quad (18)$$

$$\begin{cases} M_{\beta_n}(pT, \xi) \geq \gamma_p(pT, \xi) & \forall(n, p) \in N^2 \\ M_{\beta_n}(nT + \frac{\xi - \chi}{w}, \xi) \geq \gamma_p(nT + \frac{\xi - \chi}{w}, \xi) & \forall(n, p) \in N^2 \\ \text{s.t. } nT + \frac{\xi - \chi}{w} \in [(p-1)T, pT] \\ M_{\beta_n}(pT, \chi) \geq \beta_p(pT, \chi) & \forall(n, p) \in N^2 \end{cases} \quad (19)$$

Above all, traffic control problems can be modeled as LP formulations with linear constraints (17)-(19). In such formulations, the boundary conditions which are upstream and downstream flows are the decision variable, i.e. the objective function can be realized through controlling the inflow and outflow on a traffic link; the objective function can be any linear function of the decision variables. For a freeway link with an on-ramp, the proposed control method can be realized by on-ramp signals. For a general freeway

link without an on-ramp, some control strategies, such as dynamic tolling, have the potential to control the flows at the boundaries of the link. Although the strategies used to control the boundary flow on such a highway link are not very mature so far, it is reasonable to assume that all highway links can be controlled easily in the future.

### III. ROBUST CONTROL FOR A SINGLE HIGHWAY LINK WITH UNCERTAINTY IN INITIAL CONDITIONS

The initial conditions are known and fixed in the previous section. In reality, however, uncertainties exist in the initial conditions due to errors in the measurement. To deal with this situation, a stochastic programming model was derived where the initial conditions are random variables with normal distributions in this section. Traffic state estimation has drawn much attention in the past decades due to its contribution to reducing travel delay and ensuring travel time reliability. The normal distribution is widely used to model the uncertainties in different traffic states, such as velocity field in a CTM-v model [46], cumulative vehicle counts at the ends of a highway link [47] and traffic flow [9]. Without loss of generality, it is reasonable to approximate uncertainties in initial densities as normal distributions. However, this assumption is not necessary for our model. In fact, benefiting from the monotonicity of the Moskowitz solution, our model is applicable for all general distributions as long as the cumulative density functions are given.

#### A. The Stochastic Programming Formula

Motivated by boundary control problems, in the rest of this paper, the objective functions are only functions of boundary conditions and there are no uncertainties in the objective functions. A general inequality form of an LP problem is

$$\begin{aligned} & \text{Minimize } f(x) \\ & \text{s.t. } Ax \geq b \end{aligned} \quad (20)$$

When there is uncertainty in the constraints, we can formulate the counterpart stochastic programming problem with chance constraints, as follows:

$$\begin{aligned} & \text{Minimize } f(x) \\ & \text{s.t. } Pr\{Ax \geq b\} \geq 1 - \alpha \end{aligned} \quad (21)$$

where  $f(x)$  is a linear function of  $x$ ;  $x$  is a decision variable vector, which represents the boundary flows in this paper;  $A$  is the coefficient matrix;  $b$  is the right-hand side constraint vector and  $1 - \alpha$  is the confidence level of the chance constraint. Assume  $\rho(k)$  is subjected to a normal distribution with mean and standard deviation of  $(\rho_k, \sigma_k)$ . Then, we can convert the constraints (17)-(19) to chance constraints. For example, the constraint of

$$M_{M_k}(pT, \xi) \geq \gamma_p(pT, \xi), \quad \forall k \in K, \quad \forall p \in N \quad (22)$$

should be converted to,

$$Pr(M_{M_k}(pT, \xi) \geq \gamma_p(pT, \xi)) \geq 1 - \alpha, \quad \forall k \in K, \quad \forall p \in N \quad (23)$$

Thanks to the monotonicity and the piecewise linearity of the Moskowitz solutions, the chance constraints can be converted to linear constraints (35)-(39). The derivation of the corresponding linear constraints is shown in Appendix A. Up to this point, we have converted the problem with chance constraints into a relaxed LP problem.

It should be noticed that the fundamental diagram is empirical, and the model could be more appropriate if those variables were regarded as random variables as well. In this paper, however, we only introduced uncertainty into initial conditions because of the complexity of dealing with stochastic model parameters, which would result in a non-tractable control problem. Although the Moskowitz solutions (11)-(13) are piecewise linear functions in the initial and boundary conditions, the bilinear terms of parameters in these solutions, e.g.  $\rho_c t v_f$  in the solution (11c), make it hard to solve the traffic control problem when the uncertainty of parameters is introduced.

### B. Case Study for A Single Highway Link

We implemented our framework onto a single highway link with 4 lanes located between the PeMS vehicle detection stations 400536 and 400284 on Highway I-880 N around Hayward, CA, USA. We divided this spatial domain of 3.858 km into 6 even segments and created a temporal domain of 7 min with 21 even segments. The model parameters were defined as follows: the capacity  $C = 8000$  vph; the critical density  $\rho_c = 0.074$  /m; the free flow speed  $v_f = 30$  m/s; the jam density  $\rho_m = 0.5$  /m. Although the densities at a specific time are not directly measured, they can be inferred from the measurement of the flow and speed. Table I shows the data measured from the weekdays between 05/01/2018 and 05/31/2018, and the time interval is from 9:00 am to 10:00 am. In Table I,  $\bar{q}$  and  $\sigma(q)$  denote the mean value and standard deviation of the flow, respectively;  $\bar{v}$  and  $\sigma(v)$  represent the mean value and standard deviation of the speed, respectively. The means of the density,  $\rho_k$ , are obtained by the approximation  $\bar{q}/\bar{v}$ . For this case study, we assumed the initial densities are normally distributed, and the mean values are equal to  $\rho_k$ .

We used the IBMilogCplex solver in Matlab to solve the LPs. The International System of Units was adopted and the units were omitted in the following analysis for simplicity. Four scenarios with different standard deviations (0.003, 0.006, 0.009 and 0.012) in the initial condition segments were investigated. For each single scenario, the standard deviation in all initial condition segments were the same and denoted by  $\sigma$ , and the confidence level,  $1 - \alpha$ , was equal to 97.5%. The objective function is,

$$\begin{aligned} \max \quad & h \sum_{i=1}^{n_{max}} q_{out}(i) - \sum_{i=2}^{n_{max}} |q_{out}(i) - q_{out}(i-1)| \\ \text{s.t.} \quad & A_{model}x \geq b_{model} \\ & q_{out}(i) \geq 0 \quad \forall i \in N \end{aligned} \quad (24)$$

where the first term is to maximize the total outflow during the simulation time, and the second term smooths the outflows through forcing the difference between two adjacent outflows

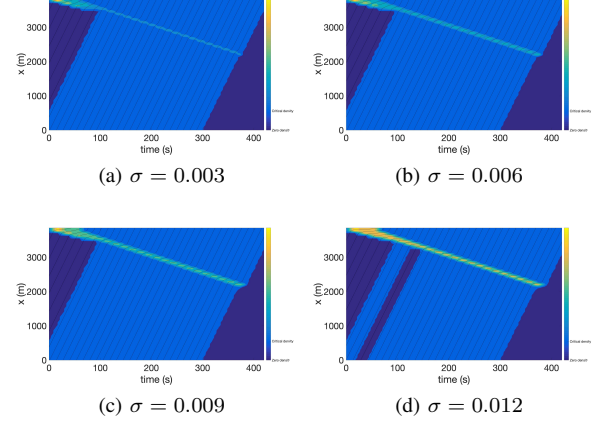


Fig. 1. Solution to robust control problem (24).

to be as small as possible.  $h > 2$  ensures that the optimally total outflow is not impacted, and the proof is shown in Appendix B.  $h = 3$  is employed in the rest of this paper.  $A_{model}$  and  $b_{model}$  are the coefficient matrix and right-hand side vector coming from the inequalities (35) to (39). The second term in the objective function was not a linear function of decision variables. To linearize the objective function, we added another variable vector  $q_d(i), i \in \{2, 3, \dots, n_{max}\}$  and extra constraints into this model,

$$\begin{aligned} \max \quad & h \sum_{i=1}^{n_{max}} q_{out}(i) - \sum_{i=2}^{n_{max}} q_d(i) \\ \text{s.t.} \quad & A_{model}x \geq b_{model} \\ & q_d(i) \geq q_{out}(i) - q_{out}(i-1), \quad \forall i \in \{2, 3, \dots, n_{max}\} \\ & q_d(i) \geq q_{out}(i-1) - q_{out}(i), \quad \forall i \in \{2, 3, \dots, n_{max}\} \\ & q_{out}(i) \geq 0 \quad \forall i \in N \end{aligned} \quad (25)$$

The Moskowitz functions corresponding to the optimal solutions are shown in Fig. 1. All of the shockwaves, which are the congested section indicated by the yellow band, are consecutive, which makes the outflow smooth without losing optimality in terms of total outflow. In these cases, the confidence level was fixed, so the confidence interval for the initial condition was wider when the standard deviation was larger. Intuitively, the chance constraints forced the solution to satisfy (17)-(19) for all of the values of the initial conditions in the confidence interval. Therefore, the wider the confidence interval was, the more restricted the feasible region was. As this is a maximization problem, the optimal value should be lower for the case with larger standard deviation (i.e. with smaller feasible region). With increasing standard deviation, the temporal width of the shock wave (the yellow band) was wider because fewer vehicles could proceed, as shown in Fig. 1.

To explore the influence of the standard deviation of the initial conditions and the confidence level on the optimal value, different scenarios with different variance and confidence levels were solved. The corresponding optimal values are shown in

TABLE I  
STATISTICS OF TRAFFIC STATES

stations	$\bar{q}$ (vph)	$\sigma(q)$ (vph)	$\bar{v}$ (m/s)	$\sigma(v)$ (m/s)	$\rho_k$ (vpm)
400536	6663.9	264.1	28.4	0.3	0.065
400488	4939.0	191.7	28.9	0.3	0.047
401561	5120.5	325.4	27.6	0.6	0.052
400611	5382.3	198.6	26.1	1.8	0.057
400928	5079.6	368.8	27.5	0.8	0.051
400284	5258.4	266.5	25.9	1.4	0.056

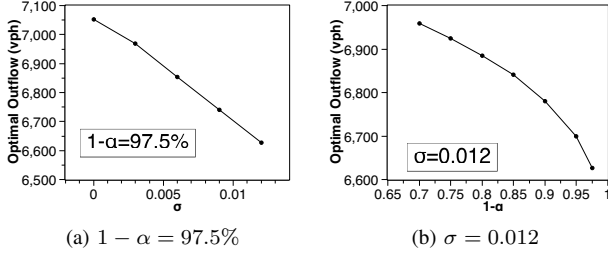


Fig. 2. Relationship between optimal total outflow and uncertainty.

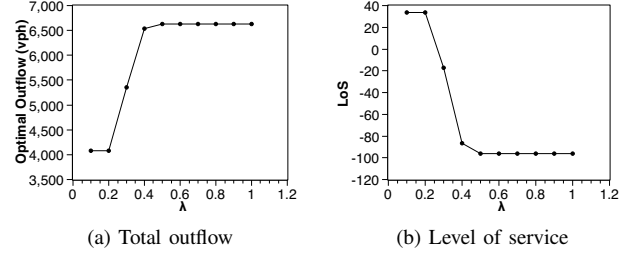


Fig. 3. Components of optimal value.

Fig. 2.

In Fig. 2(a), the confidence level is fixed, and the optimal total outflow decreases as the standard deviation of the initial conditions increases. In Fig. 2(b), the standard deviation is fixed, and the optimal total outflow decreases as the confidence level increases. The trends of these two curves can be explained by the same reason as before: as variability increases, optimal outflow decreases. For the case with a confidence level of 97.5%, when the standard deviation goes up to 0.07, the LP will become infeasible. This can be seen through Fig. 10. A large standard deviation may lead to a large  $z_{1-\alpha}$ , and the associated  $f_2(\rho_k + z_{1-\alpha}\sigma_k)$  may be zero because it was a decreasing function of  $\rho_k$ . This will generate a constraint forcing the boundary conditions to be less than zero, which will result in infeasibility. Above all, the feasible region shrinks as the variation increases.

In reality, we may not only want to maximize the outflow, but also to minimize the congestion. There are several ways to realize this objective, such as adding other constraints to represent the worst level of service and change the objective function. Here, we formulated this problem as follows:

$$\begin{aligned}
 \min \quad & -\lambda \sum_{i=1}^{n_{max}} q_{out}(i) + (1-\lambda)Q \\
 \text{s.t.} \quad & Q \geq \sum_{j=1}^i (q_{in}(j) - q_{out}(j)), \quad \forall i \in N \\
 & A_{model}x \geq b_{model} \\
 & q_{out}(i) \geq 0 \quad \forall i \in N
 \end{aligned} \quad (26)$$

where  $QT + \sum_{k=1}^{k_{max}} \rho(k)X$  is the maximum number of vehicles stuck in the link during the simulation,  $\lambda$  and  $1-\lambda$  are the weights of total outflow and  $Q$ , respectively. The sum of weighted negative total outflow and  $Q$  is the new objective function.

The standard deviation of the initial conditions was 0.012,

and the confidence level of the chance constraints was 97.5%. To make the result more intuitive, we defined the level of service as  $LoS = -QT$ . Optimal solutions for different weightings (Fig. 3) show that there is a tradeoff between outflow and the level of service. With an increase in  $\lambda$ , more vehicles can go through the highway link with a poorer level of service. When  $\lambda \geq 0.5$ , the sum of the outflows becomes dominant, and the optimal values are stable. This critical value of  $\lambda$  depends on the standard deviation of the densities and the confidence level.

#### IV. ROBUST CONTROL FOR A HIGHWAY NETWORK

The effect of the proposed robust model on a highway network shown in Fig. 4 was studied in this section. This network includes 2 highways, 6 highway links, 2 on-ramps, 2 off-ramps and 1 intersection.

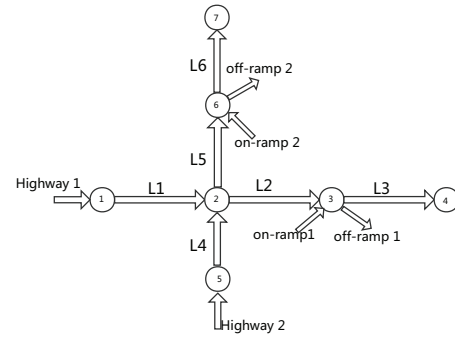


Fig. 4. Highway network layout.

### A. Network Modeling

For this network, we assume the traffic flow transition matrices at junctions are known. Then, the traffic flow at a junction with  $N_i$  incoming links and  $N_o$  outgoing links can be modeled as,

$$\begin{bmatrix} q_{out} \\ q_{off} \end{bmatrix} = \begin{bmatrix} \mathbf{P}^1 & \mathbf{P}^2 \\ \mathbf{P}^3 & 0 \end{bmatrix} \begin{bmatrix} q_{in} \\ q_{on} \end{bmatrix}, \quad (27)$$

where  $q_{in}$  and  $q_{out}$  are two column vectors denoting the incoming flows and outgoing flows at a junction node, respectively;  $q_{on}$  and  $q_{off}$  are two scalars representing the on-ramp and off-ramp flows;  $\mathbf{P}^1$  is a  $N_o \times N_i$  matrix of which each element  $\mathbf{P}^1(i, j)$  means the proportion of the vehicles from incoming link  $j$  going into link  $i$ ;  $\mathbf{P}^2$  is a column vector with dimension of  $N_o \times 1$  of which each element  $\mathbf{P}^2(i)$  means the proportion of the vehicles from on-ramp going into link  $i$ ;  $\mathbf{P}^3$  is a row vector with dimension of  $1 \times N_i$  of which each element  $\mathbf{P}^3(j)$  means the proportion of the vehicles from incoming link  $j$  departing from the off-ramp. In addition, we assumed no vehicles coming from an on-ramp would depart from the off-ramp at the same junction.

In the network shown in Fig. 4, the links 1-3 have 4 lanes, and the links 4-6 have 3 lanes. The length of each link is 1200 m and divided evenly into 2 segments. A time domain of 500 s is divided evenly into 25 segments. The free flow speed is  $v_f = 30$  m/s; the critical density is  $\rho_c = 0.0175$  /m/lane; the capacity is  $C = 1,890$  vph/lane, and the jam density is  $\rho_m = 0.1125$  /m/lane. The transition matrices are as follows,

$$\begin{aligned} \mathbf{P}_2^1 &= \begin{bmatrix} P(1, 2) & P(4, 2) \\ P(1, 5) & P(4, 5) \end{bmatrix} = \begin{bmatrix} 0.6 & 0.8 \\ 0.4 & 0.2 \end{bmatrix} \\ P_3^2 &= P_6^2 = 1 \\ P_3^3 &= P_6^3 = 0.2, \end{aligned} \quad (28)$$

The subscripts in (28) represent the junction nodes. Note the vectors  $\mathbf{P}^2$  and  $\mathbf{P}^3$  become scalars since nodes 3 and 6 only contain one incoming link and one outgoing link. In this example, we considered the heavy traffic condition during peak hours, and let the sending flows to nodes 1 and 5 equal the capacity. Corresponding to the given transition matrix (28), links 5 and 6 are uncongested while other links are congested. For simplicity, we only considered the uncertainties of link 3. To model the traffic control for this network, we need to define new notations:  $n_{lane}(i)$  denotes the number of lanes of link  $i$ ;  $V$  and  $L$  are the sets of nodes and links, respectively;  $q_{in}(i, j)$  and  $q_{out}(i, j)$  are the inflows and outflows of link  $j$  at time  $i$ . Let  $\rho_i = 4\rho_c n_{lane}(i), \forall i \in \{1, 2, 3, 4\}$ ,  $\rho_i = 0.8\rho_c n_{lane}(i), \forall i \in \{5, 6\}$  and  $\sigma_3 = 0.2\rho_3$ . The traffic control problem for this highway network was modeled as,

$$\begin{aligned} \min \quad & - \sum_{i=1}^{n_{max}} \sum_{j=1}^{n_l} (h(q_{out}(i, j) + q_{in}(i, j)) - \\ & \eta(q_{in}(i, j) - q_{out}(i, j)) - q_d^{out}(i, j) - q_d^{in}(i, j) - y(i)) \\ \text{s.t.} \quad & q_d^{out}(i, j) \geq q_{out}(i, j) - q_{out}(i-1, j), \quad \forall i \geq 2, \quad j \in L \\ & q_d^{out}(i, j) \geq q_{out}(i-1, j) - q_{out}(i, j), \quad \forall i \geq 2, \quad j \in L \\ & q_d^{in}(i, j) \geq q_{in}(i, j) - q_{in}(i-1, j), \quad \forall i \geq 2, \quad j \in L \\ & q_d^{in}(i, j) \geq q_{in}(i-1, j) - q_{in}(i, j), \quad \forall i \geq 2, \quad j \in L \\ & y(i) \geq n_{lane}(4)q_{out}(i, 1) - n_{lane}(1)q_{out}(i, 4), \quad \forall i \\ & y(i) \geq n_{lane}(1)q_{out}(i, 4) - n_{lane}(4)q_{out}(i, 1), \quad \forall i \\ & q_{on}(i, 1) \geq q_{out}(i, 2)/n_{lane}(2), \quad \forall i \in N \\ & q_{on}(i, 2) \geq q_{out}(i, 4)/n_{lane}(4), \quad \forall i \in N \\ & q_{out}(i, 3) \leq \psi'(\rho_3), \quad \forall i \in N \\ & q_{out}(i, 6) \leq \psi'(\rho_6), \quad \forall i \in N \\ & (35) - (39), \quad \forall j \in L \\ & (27), \quad \forall v \in V \\ & q_d^{out}(i, j) \geq 0, \quad q_d^{in}(i, j) \geq 0 \quad \forall i, \quad j \\ & q_{out}(i, j) \geq 0, \quad q_{in}(i, j) \geq 0 \quad \forall i, \quad j \end{aligned} \quad (29)$$

The decision variables are the inflows and outflows of each link and the flows of on-ramps and off-ramps. The first term in the objective function is to maximize both the sum of outflows and inflows over all the links; the second term is a penalty term avoiding the heavy traffic congestion at the end of the simulation, and  $\eta = 0.2$  in this example; the third and the fourth terms combined with the first four constraints are to make the flows at the boundary of each link smooth; the fifth term combined with the fifth and sixth constraints enforces: (1) the ratio of outflows between links 1 and 4 equal the ratio of their capacities when the sum of their sending flows exceeds the sum of receiving flow of links 2 and 5; (2) otherwise, the outflows of links 1 and 4 equal their sending flows, respectively. Assume the on-ramps have one lane, the seventh and eighth constraints set the outflow per lane on their merging links as the lower bound of the on-ramp inflows. We assume the densities downstream nodes 4 and 7 are equal to the mean of the initial density of links 3 and 6, respectively. The ninth and tenth constraints give the upper bounds of the receiving flow at node 4 and 7, where  $\psi'(\rho) = \rho_c v_f$  if  $\rho \leq \rho_c$ ;  $\psi'(\rho) = w(\rho - \rho_m)$  if  $\rho > \rho_c$ . Furthermore, we added (35)-(39) for each link and (27) for each node. For simplicity, instead of modeling the flows of the on-ramps through adding binary variables, we treat them as continuous variables.

Fig. 5 shows the comparison of the optimal flows of on-ramp 1 between the models with deterministic constraints and chance constraints. At the beginning part of the simulation, the on-ramp flow from the robust control model is lower; at some point afterwards, it rises to the same value as the deterministic model. This is because that, as mentioned before, when the uncertainty is considered, the percentiles of initial densities replaces the means in a part of the constraints. Therefore, there exists a shock wave on link 3 in this case due to the



sending flow constraint for link 3, and it moves backward at the congestion speed. When it reaches to the upstream node, the traffic density of link 3 is equal to the mean value of the density distribution, and the optimal on-ramp flow becomes the same as the solution of the deterministic model. Above all, the affected time interval for the on-ramp flow control due to the uncertainty of the initial densities is equal to the link length divided by the congestion speed.

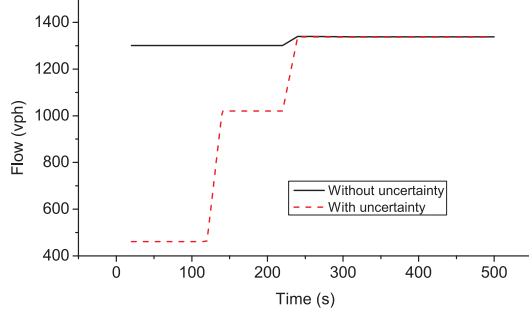


Fig. 5. Comparison of optimal flows of on-ramp 1.

Let us assume that the density of link 3 is equal to  $\rho_3 + \sigma_3$ . In the following subsections, we test the performance of the robust and non-robust models by performing forward simulations using the respective optimal inputs.

### B. On-ramp Flow Control

In this first problem, we assume that we only control the on-ramp flows in the network illustrated in Fig. 5. We assume that the inflows at link 1 and 4 are equal to the respective link capacities. The optimal outflows of the upstream links 2, 1 and 4 are shown in Fig. 6 to Fig. 7. The optimal flows from models with chance constraints are higher for all of the upstream links. Because link 2 and on-ramp 1 merge to node 3, the optimal outflow of link 2 should supplement the flow of on-ramp 2 to make the sum equal to the receiving flow of node 3. Although this change on link 2 does not induce obvious influence on the overall traffic mobility, the significance of considering the uncertainties can be seen from link 1 and link 4. Because both these two links send vehicles to link 2, they can be congested due to the congestion on link 2, and the congestion may continuously expand upstream. Quantitatively, in the robust optimal solution, although the average flow of on-ramp 1 decreases by 258 vph while the average outflows of link 1 and link 4 increase by 269 vph and 201 vph, respectively, which shows that the robust model enhances the overall mobility of this network compared to the deterministic model. Note that since we did not control the boundary inflows, the network is congested under both models. However, this example shows that the network with robust control model can accommodate higher demand than the non-robust model.

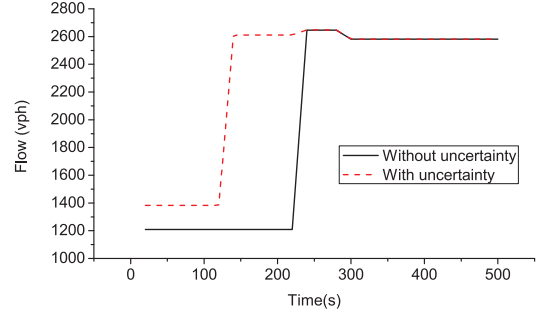


Fig. 6. Comparison of optimal outflow of link 2.

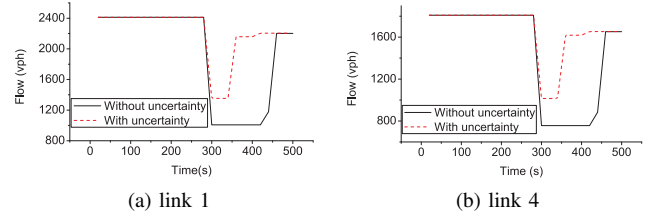


Fig. 7. Comparison of optimal outflow of links 1 and 4.

### C. Boundary Network Control (Including On-ramps)

In this problem, we control the inflows to links 1 and 4, in addition to the on-ramps, in the network of Fig. 5. The evolution of the density across all links is shown in Fig. 8. The axes denote spatial coordinates, and the unit is m. Since we fixed the on-ramp flows in this case, the flows from the on-ramps have a higher priority than the highway links to be served. At  $t = 100$ , upstream of link 2 is congested because link 3 does not have enough space to serve its sending flows. After  $t = 100$ , the robust model mitigates the congestion faster than the non-robust model. The difference between the congested areas increases with time. At the end of the simulation, the congested area of the robust case is shorter than half of the non-robust case. Therefore, the proposed model can reduce the congestion effectively.

## V. MONTE CARLO SIMULATION WITHOUT RELAXATION

### A. Difficulty without Relaxation

In the stochastic optimization model derived in the Appendix A, some constraints were relaxed, since only  $\rho(k)$  for the constraints involving  $M_{M_k}$  was considered as a random variable while all of other  $\rho(i)$ 's,  $i \in \{1, 2, \dots, k-1\}$  were regarded as fixed values with their corresponding means. In this section, the difficulty of converting the chance constraints into linear form without relaxation was explained. After this, the Monte Carlo simulation was executed to remove the relaxation. At the end of this section, the optimal objective values (total outflows) from the Monte Carlo simulation were compared to the results from the last section. For simplicity,



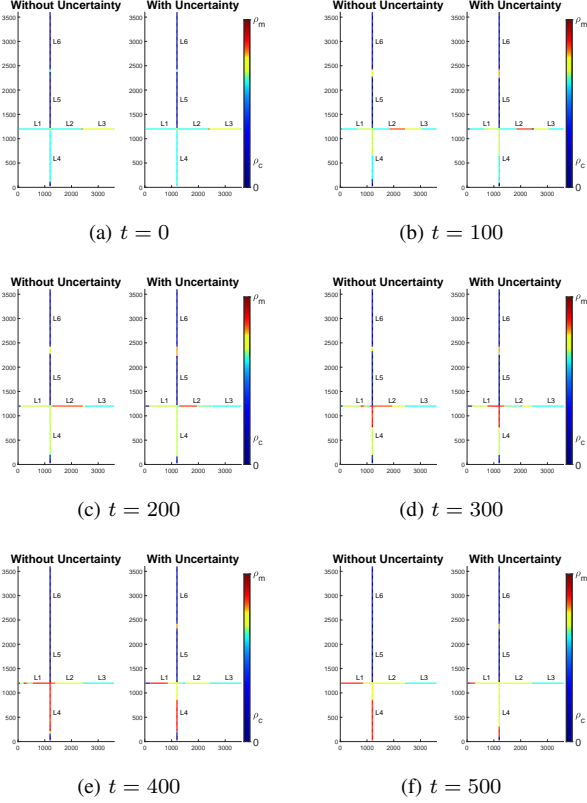


Fig. 8. Evolution of the density across the network, with classical control (left) and robust control (right).

the Moskowitz solutions from the initial conditions (11) can be expressed as:

$$M_{M_k}(t, x) = \begin{cases} f_1(\rho(i)), & \text{if } \rho(k) \geq \rho_c, i = 1, 2, \dots, K_{max} \\ f_2(\rho(i)), & \text{if } \rho(k) < \rho_c, i = 1, 2, \dots, K_{max} \end{cases} \quad (30)$$

where  $f_1$  and  $f_2$  indicate two linear functions and  $K_{max}$  is the number of the initial condition segments. As a result, the typical chance constraint involving  $M_{M_k}$  can be expressed as,

$$\begin{aligned} & Pr(M_{M_k}(t, x) \geq g(q)) \\ &= Pr(f_1(\rho(i)) \geq g(q), \rho(k) \geq \rho_c) \\ &+ Pr(f_2(\rho(i)) \geq g(q), \rho(k) < \rho_c) \end{aligned} \quad (31)$$

where  $g$  is a linear function of boundary conditions.

If all of the initial conditions are independently normally distributed,  $(f(\rho(i)), \rho(k))$  is subject to a bivariate normal distribution  $n(\mu, \Sigma)$ ,

$$\begin{aligned} \mu &= [\mu_{f(\rho(i))}, \mu_{\rho(k)}], \\ \Sigma &= \begin{bmatrix} Var(f(\rho(i))) & Cov(f(\rho(i)), \rho(k)) \\ Cov(f(\rho(i)), \rho(k)) & Var(\rho(k)) \end{bmatrix} \end{aligned} \quad (32)$$

Although the pdf of a bivariate normal distribution can be obtained, there is no closed-form of the corresponding cumulative distribution function (cdf). In fact, there is no closed-form for the cdf of an univariate normal distribution either. The integral of a normal pdf is an error function, which cannot be expressed analytically. The reason why we can convert the chance constraint into linear form is that the

normal table is available. Unfortunately, for a bivariate normal distribution, the chance constraints cannot be expressed as linear constraints by the same method.

### B. Monte Carlo Simulation

To validate our relaxed model, Monte Carlo simulations were used to convert the chance constraints into a linear form. The algorithm for constraints  $Pr(M_{M_k}(t, x) \geq \gamma(t, x)) \geq 1 - \alpha$  is as follows.

*Step 1.* Generate  $N$  random numbers from the normal distribution for each initial condition segment. In this paper,  $N = 1000$  and  $\rho(k_i)$  is the  $i$ th number for the  $k$ th segment.

*Step 2.* Calculate  $M_{M_k(i)}(t, x), i = 1, 2, \dots, N$  using the  $i$ th number from each segment from Step 1.

*Step 3.* Sort  $M_{M_k(i)}(t, x)$  into ascending order. Find the corresponding critical value. For example, if the confidence level is 97.5%, then the critical value should be  $M_{M_k(25)}(t, x)$  in the ordered sequence.

*Step 4.* Replace the constraints involving  $M_{M_k}$  and  $\gamma$  of  $Pr(M_{M_k}(t, x) \geq \gamma(t, x)) \geq 1 - \alpha$  with  $M_{M_k(N\alpha)}(t, x) \geq \gamma(t, x)$ .

Because the downstream condition of  $\beta_n(t, x)$  is a function of the initial conditions, the algorithm for the constraints  $Pr(M_{M_k}(t, x) \geq \beta(t, x)) \geq 1 - \alpha$  is as follows.

*Step 1.* Generate  $N$  random numbers from the normal distribution for each initial condition segment.  $\rho(k_i)$  is the  $i$ th number for the  $k$ th segment.

*Step 2.* Calculate  $M_{M_k(i)}(t, x) + \sum_{k=1}^{k=K_{max}} \rho(k_i)X, i = 1, 2, \dots, N$  using the  $i$ th number from each segment from Step 1.

*Step 3.* Sort  $M_{M_k(i)}(t, x) + \sum_{k=1}^{k=K_{max}} \rho(k_i)X$  in an ascending order. Use  $(M_{M_k}(t, x) + \sum_{k=1}^{k=K_{max}} \rho(k)X)_{N\alpha}$  to represent the  $N\alpha$ th element in the ordered sequence.

*Step 4.* Replace the constraints involving  $M_{M_k}$  and  $\beta$  of  $Pr(M_{M_k}(t, x) \geq \beta(t, x)) \geq 1 - \alpha$  with  $(M_{M_k}(t, x) + \sum_{k=1}^{k=K_{max}} \rho(k)X)_{N\alpha} \geq \beta(t, x) + \sum_{k=1}^{k=K_{max}} \rho(k)X$ . There is no need to modify any constraints not involving  $M_{M_k}(t, x)$  because there is no relaxation in those constraints. Since there is no constraint for the capacity downstream, the time period in which the outflow is impacted by the initial density could be approximated by the link length divided by the free flow speed, which is 7 steps in this example. The comparison of averaged outflow over this impacted time period for the problem (24) is shown in Fig. 9.

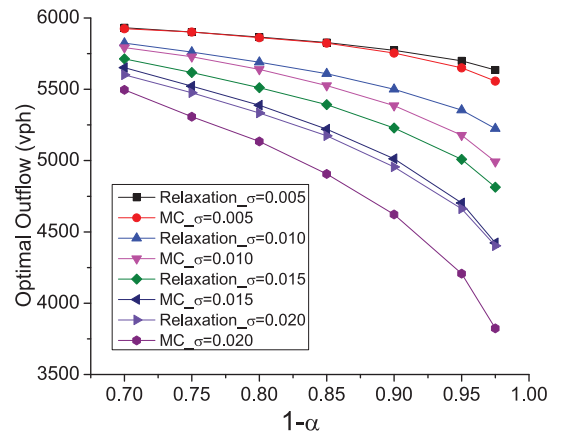


Fig. 9. Comparison of optimally total outflows.

Since the objective function is to maximize the total outflows, the optimal value from Monte Carlo simulation is smaller than the relaxed LP. The error increases with the confidence level and the standard deviation, and the largest error percent is 15%. Therefore, our relaxed stochastic program fits well with the Monte Carlo simulation. To explain the reason why the optimal solution from the relaxed LP has such a high accuracy, let us delve into some constraints. The errors that originated from the relaxed constraints are mitigated by these accurate constraints. (36) shows that, compared to the Monte Carlo simulation, the relaxed constraints generate a larger upper bound on the total outflows, and this could lead to an error

approximating  $\frac{z_{1-\alpha} \sqrt{\sum_{i=k+1}^{k_{max}} \sigma^2(i)}}{\sum_{i=k+1}^{k_{max}} \rho(i) + z_{1-\alpha} \sqrt{\sum_{i=k+1}^{k_{max}} \sigma^2(i)}}$  in percentage.

Although the constraints (35)-(37) are relaxed, the constraints (38)-(39) are accurate. For example, when  $n = 1$ ,  $p = 7$ , and the first constraint in (38) could be written as

$$-q_{in}(1)(0.57T) + \sum_{i=1}^7 q_{out}(i)T \leq \left( \sum_{k=1}^{k_{max}} \rho_k - z_{1-\alpha} \sqrt{\sum_{k=1}^{k_{max}} \sigma_k^2} \right) \quad (33)$$

This constraint is accurate and produces a stricter upper bound. Therefore, the couple effect of these constraints ensures the accuracy of our model.

## VI. CONCLUSION

In this paper, we explored a robust traffic control problem involving uncertainty in the initial densities. First, we derived a relaxed version of LP when we considered uncertainty in the initial conditions. Under this framework, this robust control problem can be solved efficiently. Following this, case studies for both a single highway link and a network show the benefits of the proposed model. In addition, Monte Carlo simulation was used to verify the accuracy of the relaxed LP.

A set of individual chance constraints was used for this framework. In future work, considering joint chance constraints is a promising topic. In addition, finding a stochastic programming formulation to deal with the uncertainty in model parameters will be another interesting research direction.

## VII. APPENDIX

### A. Linear expression of the chance constraints

The following procedure shows the derivation of the deterministic version for the chance constraint  $Pr\{M_{M_k}(pT, \xi) \geq \gamma_p(pT, \xi)\} \geq 1 - \alpha$  in detail, and the integrated deterministic constraints were obtained using the same method.

From (11), the Moskowitz solution upstream from the initial condition (6) can be explicitly expressed as:

$$M_{M_k}(t, \xi) = \begin{cases} +\infty, & \text{if } t \leq \frac{\xi - (k-1)X}{w} \\ -\sum_{i=1}^{k-1} \rho(i)X + \rho_c(tv_f + (k-1)X - \xi), & \text{if } t \geq \frac{\xi - (k-1)X}{w} \text{ and } \rho(k) \leq \rho_c \\ -\sum_{i=1}^{k-1} \rho(i)X + \rho(k)(tw + (k-1)X - \xi) \\ -\rho_m tw, & \text{if } \frac{\xi - (k-1)X}{w} \leq t \leq \frac{\xi - kX}{w} \text{ and } \rho(k) \geq \rho_c \\ -\sum_{i=1}^k \rho(i)X + \rho_c(tw + kX - \xi) - \rho_m tw, & \text{if } t \geq \frac{\xi - kX}{w} \text{ and } \rho(k) \geq \rho_c \end{cases} \quad (34)$$

From (34), it is known that  $M_{M_k}(t, \xi)$  is a nonincreasing and piecewise linear function of  $\rho(k)$ , as shown in Fig. 10. Then the corresponding chance constraint was simply divided into two situations:

(i).  $\rho_c \leq \rho_k + z_{1-\alpha}\sigma_k$  as shown left in Fig. 10. We should convert the chance constraint to  $f_2(\rho_k + z_{1-\alpha}\sigma_k) \geq \gamma_p(pT, \xi) \quad \forall k \in K, \quad \forall p \in N$ ;

(ii).  $\rho_c \geq \rho_k + z_{1-\alpha}\sigma_k$  as shown right in Fig. 10. We should convert the chance constraint to  $f_1(\rho_k + z_{1-\alpha}\sigma_k) \geq \gamma_p(pT, \xi) \quad \forall k \in K, \quad \forall p \in N$ .

where  $z_{1-\alpha}$  is defined as z score such that  $P(\rho(k) \leq \rho_k + z_{1-\alpha}\sigma_k) = 1 - \alpha$ .

Substituting the expressions of  $M_{M_k}(t, \xi)$  (34) and  $\gamma_p(pT, \xi)$

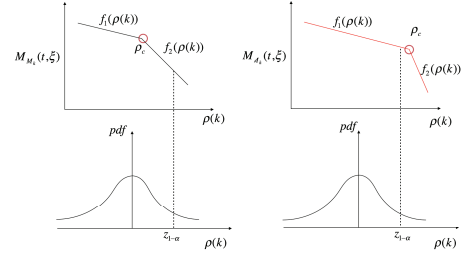


Fig. 10. Solution at upstream from initial condition and associated initial density distribution.

(7) into the inequalities above leads to the following linear and deterministic constraint:

$$\begin{cases} -\sum_{i=1}^{k-1} \rho(i)x + \rho_c(pTv_f + (k-1)x - \xi) \\ \geq \sum_{i=1}^p q_{in}(i)T, & \text{if } t \geq \frac{\xi - (k-1)X}{w} \\ & \text{and } \rho_k + z_{1-\alpha}\sigma_k \leq \rho_c \\ -\sum_{i=1}^{k-1} \rho(i)X + (\rho(k) + z_{1-\alpha}\sigma_k)(tw + (k-1)X - \xi) \\ -\rho_m tw \geq \sum_{i=1}^p q_{in}(i)T, & \text{if } \frac{\xi - (k-1)X}{w} \leq t \leq \frac{\xi - kX}{w}, \\ & \text{and } \rho_k + z_{1-\alpha}\sigma_k \geq \rho_c \\ -\sum_{i=1}^{k-1} \rho(i)X - (\rho(k) + z_{1-\alpha}\sigma_k)X + \rho_c(tw + kX - \xi) \\ -\rho_m tw \geq \sum_{i=1}^p q_{in}(i)T, & \text{if } t \geq \frac{\xi - kX}{w}, \\ & \text{and } \rho_k + z_{1-\alpha}\sigma_k \geq \rho_c \end{cases} \quad (35)$$

For simplicity, only  $\rho(k)$  for the constraints involving  $M_{M_k}$  was considered as a random variable, all other  $\rho(i)'s, i \in \{1, 2, \dots, k-1\}$  were still regarded as fixed values with their corresponding means. In section 4, the complexity of regarding all of the  $\rho(i)'s, i \in \{1, 2, \dots, k-1\}$  as random variables will be explained.

The other constraints were found in this same manner. The deterministic expression for the rest of the constraints in (17) is shown in (36) and (37), and the deterministic expression of

(18) and (19) are shown in (38) and (39), respectively,

$$(36) \quad \left\{ \begin{array}{ll} \sum_{i=k+1}^{k_{max}} \rho(i)X + (\rho_k - z_{1-\alpha}\sigma_k)(pTv_f + kX - \chi) \\ \geq \sum_{i=1}^p q_{out}(i)T, & \text{if } \frac{\chi - kX}{v_f} \leq pT \leq \frac{\chi - (k-1)X}{v_f}, \\ & \text{and } \rho_k - z_{1-\alpha}\sigma_k \leq \rho_c \\ \sum_{i=k+1}^{k_{max}} \rho(i)X + (\rho_k - z_{1-\alpha}\sigma_k)X + \\ \rho_c(pTv_f + (k-1)X - \chi) \\ \geq \sum_{i=1}^p q_{out}(i)T, & \text{if } pT \geq \frac{\chi - (k-1)X}{v_f}, \\ & \text{and } \rho_k - z_{1-\alpha}\sigma_k \leq \rho_c \\ \sum_{i=k+1}^{k_{max}} \rho(i)X + \rho_c(pTv_f + kX - \chi) - \rho_m pTw \\ \geq \sum_{i=1}^p q_{out}(i)T, & \text{if } pT \geq \frac{\chi - kX}{v_f}, \\ & \text{and } \rho_k - z_{1-\alpha}\sigma_k \geq \rho_c \end{array} \right.$$

$$(37) \quad \left\{ \begin{array}{ll} -\sum_{i=1}^{k-1} \rho_i x + \rho_c \left( \frac{\xi - (k-1)X}{w} v_f + (k-1)x - \xi \right) \\ \geq \sum_{i=1}^{p-1} q_{in}(i)T + q_{in}(p) \left( \frac{\xi - (k-1)X}{w} - (p-1)T \right), \\ & \text{if } (p-1)T \leq \frac{\xi - (k-1)X}{w} \leq pT, \\ & \text{and } \rho_k + z_{1-\alpha}\sigma_k \leq \rho_c \\ -\sum_{i=1}^{k-1} \rho_i x - \rho_m (\xi - (k-1)X) \\ \geq \sum_{i=1}^{p-1} q_{in}(i)T + q_{in}(p) \left( \frac{\xi - (k-1)X}{w} - (p-1)T \right), \\ & \text{if } (p-1)T \leq \frac{\xi - (k-1)X}{w} \leq pT, \\ & \text{and } \rho_k + z_{1-\alpha}\sigma_k \geq \rho_c \\ \sum_{i=k+1}^{k_{max}} \rho_i x \\ \geq \sum_{i=1}^{p-1} q_{out}(i)T + q_{out}(p) \left( \frac{\chi - kX}{v_f} - (p-1)T \right), \\ & \text{if } (p-1)T \leq \frac{\chi - kX}{v_f} \leq pT, \\ & \text{and } \rho_k + z_{1-\alpha}\sigma_k \leq \rho_c \\ \sum_{i=k+1}^{k_{max}} \rho_i x + \rho_c \left( \frac{\chi - kX}{v_f} w + kX - \chi \right) \\ \geq \sum_{i=1}^{p-1} q_{out}(i)T + q_{out}(p) \left( \frac{\chi - kX}{v_f} - (p-1)T \right), \\ & \text{if } (p-1)T \leq \frac{\chi - kX}{v_f} \leq pT, \\ & \text{and } \rho_k + z_{1-\alpha}\sigma_k \geq \rho_c \end{array} \right.$$

$$(38) \quad \left\{ \begin{array}{ll} -\sum_{i=1}^{n-1} q_{in}(i)T - q_{in}(n)(pT - \frac{\chi - \xi}{v_f} - (n-1)T) \\ + \sum_{i=1}^p q_{out}(i)T \leq (\sum_{k=1}^{k_{max}} \rho_k - z_{1-\alpha} \sqrt{\sum_{k=1}^{k_{max}} \sigma_k^2})X \\ & \text{if } (n-1)T + \frac{\chi - \xi}{v_f} \leq pT \leq nT + \frac{\chi - \xi}{v_f} \\ -\sum_{i=1}^n q_{in}(i)T - \rho_c v_f (pT - \frac{\chi - \xi}{v_f} - nT) + \sum_{i=1}^p q_{out}(i)T \\ \leq (\sum_{k=1}^{k_{max}} \rho_k - z_{1-\alpha} \sqrt{\sum_{k=1}^{k_{max}} \sigma_k^2})X \\ & \text{if } pT \geq nT + \frac{\chi - \xi}{v_f} \\ -\sum_{i=1}^n q_{in}(i)T + \sum_{i=1}^{p-1} q_{out}(i)T \\ + q_{out}(p)(nT + \frac{\chi - \xi}{v_f} - (p-1)T) \\ \leq (\sum_{k=1}^{k_{max}} \rho_k - z_{1-\alpha} \sqrt{\sum_{k=1}^{k_{max}} \sigma_k^2})X \\ & \text{if } (p-1)T \leq nT + \frac{\chi - \xi}{v_f} \leq pT \end{array} \right.$$

$$(39) \quad \left\{ \begin{array}{ll} \sum_{i=1}^{n-1} q_{out}(i)T + q_{out}(n)(pT - \frac{\xi - \chi}{w} - (n-1)T) \\ - \rho_m (\xi - \chi) - \sum_{i=1}^p q_{in}(i)T \\ \geq (\sum_{k=1}^{k_{max}} \rho_k + z_{1-\alpha} \sqrt{\sum_{k=1}^{k_{max}} \sigma_k^2})X \\ & \text{if } (n-1)T + \frac{\xi - \chi}{w} \leq pT \leq nT + \frac{\xi - \chi}{w} \\ \sum_{i=1}^n q_{out}(i)T + \rho_c v_f (pT - \frac{\xi - \chi}{w} - nT) \\ - \sum_{i=1}^{p-1} q_{in}(i)T \\ \geq (\sum_{k=1}^{k_{max}} \rho_k + z_{1-\alpha} \sqrt{\sum_{k=1}^{k_{max}} \sigma_k^2})X \\ & \text{if } pT \geq nT + \frac{\xi - \chi}{w} \\ \sum_{i=1}^n q_{out}(i)T + \rho_c v_f (\frac{\xi - \chi}{w} - \frac{\xi - \chi}{v_f}) \\ - \sum_{i=1}^{p-1} q_{in}(i)T + q_{in}(p)(nT + \frac{\xi - \chi}{w} - (p-1)T) \\ \geq (\sum_{k=1}^{k_{max}} \rho_k + z_{1-\alpha} \sqrt{\sum_{k=1}^{k_{max}} \sigma_k^2})X \\ & \text{if } (p-1)T \leq nT + \frac{\xi - \chi}{w} \leq pT \end{array} \right.$$

## B. Proof of the relationship between the total outflow and the differentials of outflows across time steps

Assume  $q'_{out}(i)$  is the optimal solution of the objective function  $\max \sum_{i=1}^{n_{max}} q_{out}(i)$ . For any feasible solution of (24), the objective function is

$$(40) \quad \sum_{i \in Q^{++}} (h+2)q_{out}(i) + \sum_{i \in Q^+} (h+1)q_{out}(i) + \sum_{i \in Q} hq_{out}(i) + \sum_{i \in Q^-} (h-1)q_{out}(i) + \sum_{i \in Q^{--}} (h-2)q_{out}(i)$$

where

$$(41) \quad Q^{++} = \{i : q_{out}(i) < q_{out}(i+1) \cap q_{out}(i) < q_{out}(i-1)\}$$

$$(42) \quad Q^+ = \{i : q_{out}(i) < q_{out}(i+1) \cap q_{out}(i) = q_{out}(i-1) \text{ or } q_{out}(i) = q_{out}(i+1) \cap q_{out}(i) < q_{out}(i-1)\}$$

$$(43) \quad Q^{--} = \{i : q_{out}(i) > q_{out}(i+1) \cap q_{out}(i) > q_{out}(i-1)\}$$

$$(44) \quad Q^- = \{i : q_{out}(i) > q_{out}(i+1) \cap q_{out}(i) = q_{out}(i-1) \text{ or } q_{out}(i) = q_{out}(i+1) \cap q_{out}(i) > q_{out}(i-1)\}$$

$$(45) \quad Q = \{i : i \in I - Q^{++} - Q^+ - Q^{--} - Q^-\}$$

$q_{out}(1)$  and  $q_{out}(n_{max})$  are in  $Q^+$ ,  $Q$  or  $Q^-$  based on the same logic. When  $h > 2$ , the coefficient for any time step  $i$  is positive. Assume the optimal solution of (40) is  $q^*_{out}(i)$  and the total outflow  $\sum_{i=1}^{n_{max}} q^*_{out}(i)$  is less than  $\sum_{i=1}^{n_{max}} q'_{out}(i)$ , there must exist at least one time step such that  $q^*_{out}(i) < q'_{out}(i)$ . Since the coefficients are all positive, let  $q'_{out}(i)$  replace  $q^*_{out}(i)$ , the new objective value of (40) will be larger than  $\sum_{i=1}^{n_{max}} q^*_{out}(i)$ . Therefore,  $q^*_{out}(i)$  is not the optimal solution. Therefore, the optimally total outflow of  $\sum_{i=1}^{n_{max}} q^*_{out}(i)$  equals  $\sum_{i=1}^{n_{max}} q'_{out}(i)$ .

## REFERENCES

- [1] M. J. Lighthill and G. B. Whitham, "On kinematic waves. ii. a theory of traffic flow on long crowded roads," in *Proceedings of the Royal Society of London A: Mathematical, Physical and Engineering Sciences*, vol. 229, no. 1178. The Royal Society, 1955, pp. 317–345.
- [2] P. I. Richards, "Shock waves on the highway," *Operations research*, vol. 4, no. 1, pp. 42–51, 1956.
- [3] A. Aw and M. Rascle, "Resurrection of" second order" models of traffic flow," *SIAM journal on applied mathematics*, vol. 60, no. 3, pp. 916–938, 2000.
- [4] S. Blandin, D. Work, P. Goatin, B. Piccoli, and A. Bayen, "A general phase transition model for vehicular traffic," *SIAM journal on Applied Mathematics*, vol. 71, no. 1, pp. 107–127, 2011.
- [5] D. C. Gazis and C. H. Knapp, "On-line estimation of traffic densities from time-series of flow and speed data," *Transportation Science*, vol. 5, no. 3, pp. 283–301, 1971.
- [6] D. Gazis and C. Liu, "Kalman filtering estimation of traffic counts for two network links in tandem," *Transportation Research Part B: Methodological*, vol. 37, no. 8, pp. 737–745, 2003.

- [7] H. Wang, J. Li, Q.-Y. Chen, and D. Ni, "Speed-density relationship: From deterministic to stochastic," in *The 88th Transportation Research Board (TRB) Annual Meeting*. Washington, DC, 2009.
- [8] M. W. Szeto and D. C. Gazis, "Application of Kalman filtering to the surveillance and control of traffic systems," *Transportation Science*, vol. 6, no. 4, pp. 419–439, 1972.
- [9] Y. Wang and M. Papageorgiou, "Real-time freeway traffic state estimation based on extended Kalman filter: a general approach," *Transportation Research Part B: Methodological*, vol. 39, no. 2, pp. 141–167, 2005.
- [10] Y. Wang, M. Papageorgiou, and A. Messmer, "Real-time freeway traffic state estimation based on extended Kalman filter: A case study," *Transportation Science*, vol. 41, no. 2, pp. 167–181, 2007.
- [11] S. E. Jabari and H. X. Liu, "A stochastic model of traffic flow: Theoretical foundations," *Transportation Research Part B: Methodological*, vol. 46, no. 1, pp. 156–174, 2012.
- [12] L. Zhang, J. Ma, and C. Zhu, "Theory modeling and application of an adaptive Kalman filter for short-term traffic flow prediction," *Journal of Information and Computational Science*, vol. 9, no. 16, pp. 5101–5109, 2012.
- [13] M.-C. Tan, L.-B. Feng, and J.-M. Xu, "Traffic flow prediction based on hybrid arima and ann model," *Zhongguo Gonglu Xuebao (China Journal of Highway and Transport)*, vol. 20, no. 4, pp. 118–121, 2007.
- [14] R. Bauza and J. Gozávez, "Traffic congestion detection in large-scale scenarios using vehicle-to-vehicle communications," *Journal of Network and Computer Applications*, vol. 36, no. 5, pp. 1295–1307, 2013.
- [15] J. Rzeszútó and S. H. Nguyen, "Machine learning for traffic prediction," *Fundamenta Informaticae*, vol. 119, no. 3–4, pp. 407–420, 2012.
- [16] L. Jia, L. Yang, Q. Kong, and S. Lin, "Study of artificial immune clustering algorithm and its applications to urban traffic control," *International Journal of Information Technology*, vol. 12, no. 3, pp. 1–6, 2006.
- [17] P. Lopez-Garcia, E. Onieva, E. Osaba, A. D. Masegosa, and A. Perallos, "A hybrid method for short-term traffic congestion forecasting using genetic algorithms and cross entropy," *IEEE Transactions on Intelligent Transportation Systems*, vol. 17, no. 2, pp. 557–569, 2016.
- [18] C. Pasquale, I. Papamichail, C. Roncoli, S. Saccone, S. Siri, and M. Papageorgiou, "Two-class freeway traffic regulation to reduce congestion and emissions via nonlinear optimal control," *Transportation Research Part C: Emerging Technologies*, vol. 55, pp. 85–99, 2015.
- [19] D. Pisarski and C. Canudas-de Wit, "Nash game-based distributed control design for balancing traffic density over freeway networks," *IEEE Transactions on Control of Network Systems*, vol. 3, no. 2, pp. 149–161, 2016.
- [20] Y. Li, E. Canepa, and C. Claudel, "Optimal control of scalar conservation laws using linear/quadratic programming: Application to transportation networks," *IEEE Transactions on Control of Network Systems*, vol. 1, no. 1, pp. 28–39, 2014.
- [21] M. Papageorgiou, H. Hadj-Salem, and J.-M. Blosseville, "Alinea: A local feedback control law for on-ramp metering," *Transportation Research Record*, vol. 1320, no. 1, pp. 58–67, 1991.
- [22] G. Gomes and R. Horowitz, "Optimal freeway ramp metering using the asymmetric cell transmission model," *Transportation Research Part C: Emerging Technologies*, vol. 14, no. 4, pp. 244–262, 2006.
- [23] A. Kotsialos, M. Papageorgiou, M. Mangeas, and H. Haj-Salem, "Coordinated and integrated control of motorway networks via non-linear optimal control," *Transportation Research Part C: Emerging Technologies*, vol. 10, no. 1, pp. 65–84, 2002.
- [24] X.-Y. Lu, P. Varaiya, and R. Horowitz, "An equivalent second order model with application to traffic control," *IFAC Proceedings Volumes*, vol. 42, no. 15, pp. 375–382, 2009.
- [25] R. C. Carlson, I. Papamichail, and M. Papageorgiou, "Local feedback-based mainstream traffic flow control on motorways using variable speed limits," *IEEE Transactions on Intelligent Transportation Systems*, vol. 12, no. 4, pp. 1261–1276, 2011.
- [26] M. Gugat, M. Herty, A. Klar, and G. Leugering, "Optimal control for traffic flow networks," *Journal of optimization theory and applications*, vol. 126, no. 3, pp. 589–616, 2005.
- [27] C. C. De Wit, "Best-effort highway traffic congestion control via variable speed limits," in *Decision and Control and European Control Conference (CDC-ECC), 2011 50th IEEE Conference on*. IEEE, 2011, pp. 5959–5964.
- [28] F. Morbidi, L. L. Ojeda, C. C. De Wit, and I. Bellicot, "A new robust approach for highway traffic density estimation," in *Control Conference (ECC), 2014 European*. IEEE, 2014, pp. 2575–2580.
- [29] A. A. Kurzhanskiy and P. Varaiya, "Guaranteed prediction and estimation of the state of a road network," *Transportation research part C: emerging technologies*, vol. 21, no. 1, pp. 163–180, 2012.
- [30] C. M. Tampère and L. Immers, "An extended Kalman filter application for traffic state estimation using CTM with implicit mode switching and dynamic parameters," in *Intelligent Transportation Systems Conference, 2007. ITSC 2007. IEEE*. IEEE, 2007, pp. 209–216.
- [31] A. Hegyi, D. Girimonte, R. Babuska, and B. De Schutter, "A comparison of filter configurations for freeway traffic state estimation," in *Intelligent Transportation Systems Conference, 2006. ITSC'06. IEEE*. IEEE, 2006, pp. 1029–1034.
- [32] G. Dervisoglu, G. Gomes, J. Kwon, R. Horowitz, and P. Varaiya, "Automatic calibration of the fundamental diagram and empirical observations on capacity," in *Transportation Research Board 88th Annual Meeting*, vol. 15, 2009.
- [33] A. Polus and M. A. Pollatschek, "Stochastic nature of freeway capacity and its estimation," *Canadian Journal of Civil Engineering*, vol. 29, no. 6, pp. 842–852, 2002.
- [34] K. Ozbay and E. E. Ozguven, "A comparative methodology for estimating the capacity of a freeway section," in *Intelligent Transportation Systems Conference, 2007. ITSC 2007. IEEE*. IEEE, 2007, pp. 1034–1039.
- [35] Y. Li, E. Canepa, and C. Claudel, "Exact solutions to robust control problems involving scalar hyperbolic conservation laws using mixed integer linear programming," in *Communication, Control, and Computing (Allerton), 2013 51st Annual Allerton Conference on*. IEEE, 2013, pp. 478–485.
- [36] C. G. Claudel and A. M. Bayen, "Convex formulations of data assimilation problems for a class of Hamilton-Jacobi equations," *SIAM Journal on Control and Optimization*, vol. 49, no. 2, pp. 383–402, 2011.
- [37] P.-E. Mazaré, A. H. Dehwh, C. G. Claudel, and A. M. Bayen, "Analytical and grid-free solutions to the lighthill-whitham-richards traffic flow model," *Transportation Research Part B: Methodological*, vol. 45, no. 10, pp. 1727–1748, 2011.
- [38] E. S. Canepa and C. G. Claudel, "Exact solutions to traffic density estimation problems involving the Lighthill-Whitham-Richards traffic flow model using mixed integer programming," in *Intelligent Transportation Systems (ITSC), 2012 15th International IEEE Conference on*. IEEE, 2012, pp. 832–839.
- [39] —, "Spoofing cyber attack detection in probe-based traffic monitoring systems using mixed integer linear programming," in *Computing, Networking and Communications (ICNC), 2013 International Conference on*. IEEE, 2013, pp. 327–333.
- [40] K. Moskowitz, "Discussion of 'freeway level of service as influenced by volume and capacity characteristics' by DR Drew and CJ Keese," *Highway Research Record*, vol. 99, pp. 43–44, 1965.
- [41] E. Barron and R. Jensen, "Semicontinuous viscosity solutions for Hamilton-Jacobi equations with convex Hamiltonians," *Communications in Partial Differential Equations*, vol. 15, no. 12, pp. 293–309, 1990.
- [42] H. Frankowska, "Lower semicontinuous solutions of Hamilton-Jacobi-Bellman equations," *SIAM Journal on Control and Optimization*, vol. 31, no. 1, pp. 257–272, 1993.
- [43] J.-P. Aubin, A. M. Bayen, and P. Saint-Pierre, "Dirichlet problems for some Hamilton-Jacobi equations with inequality constraints," *SIAM Journal on Control and Optimization*, vol. 47, no. 5, pp. 2348–2380, 2008.
- [44] C. G. Claudel and A. M. Bayen, "Lax-Hopf based incorporation of internal boundary conditions into Hamilton-Jacobi equation. part i: Theory," *IEEE Transactions on Automatic Control*, vol. 55, no. 5, pp. 1142–1157, 2010.
- [45] —, "Lax-Hopf based incorporation of internal boundary conditions into Hamilton-Jacobi equation. part ii: Computational methods," *IEEE Transactions on Automatic Control*, vol. 55, no. 5, pp. 1158–1174, 2010.
- [46] D. B. Work, O.-P. Tossavainen, S. Blandin, A. M. Bayen, T. Iwuchukwu, and K. Tracton, "An ensemble Kalman filtering approach to highway traffic estimation using GPS enabled mobile devices," in *Decision and Control, 2008. CDC 2008. 47th IEEE Conference on*. IEEE, 2008, pp. 5062–5068.
- [47] W. Deng, H. Lei, and X. Zhou, "Traffic state estimation and uncertainty quantification based on heterogeneous data sources: A three detector approach," *Transportation Research Part B: Methodological*, vol. 57, pp. 132–157, 2013.